

## **Supporting online material**

### **Materials and Methods**

*Gene synthesis, mutagenesis and screening.* A gene encoding IFP1.0 with codons optimized for *Escherichia coli* was synthesized by overlap extension PCR (*S1*). Genetic libraries were constructed by saturation and random mutagenesis as described (*S2*) and DNA shuffling (*S3*). IFP1.0 and mutants were cloned into a modified pBAD vector containing the heme oxygenase-1 gene from cyanobacteria. Libraries were expressed and screened as described (*S2*). A 676 nm laser was used for FACS screening of large libraries, with 710 – 900 nm emission filter.

*Protein expression and characterization.* IFPs in the modified pBAD vector were expressed in *E. coli* strain TOP10. Protein purification, fluorescence characterization and photobleaching experiments were done as described (*S2*). For quantum yield determinations, the integral of the emission spectrum (corrected for the wavelength-dependence of detection sensitivity) of a solution of IFP in PBS was compared with the analogous integral for an equally absorbing solution of Cy5 in PBS, whose quantum yield was assumed to be 0.27 (*S4*). For extinction coefficient determination, the holoprotein concentration was calculated based on the assumption that the extinction coefficient of holoprotein at 388 nm was equal to that of free BV, which was measured to be 39,900 M<sup>-1</sup> cm<sup>-1</sup> in PBS. This is based on the result that the absorbance by the Q band (670 – 700 nm) decreased by ~ 10 fold after denaturation while the absorbance at 388 nm did not change.

*Chimera construction and imaging.* DNA encoding IFP1.0 with codons optimized for mammals was synthesized by overlap extension PCR (*SI*). Other IFPs were created by QuickChange Multi site-directed mutagenesis. AKT1's PH domain was fused to the c-terminus of IFP1.4 to generate chimeras IFP1.4-PH<sup>AKT1</sup>. All the IFPs and chimera were cloned into pcDNA3.1 vector. HEK293A cells were transfected with IFP cDNAs using Fugene, then imaged 24-48 hr later on a Zeiss Axiovert microscope with redshifted Cy5.5 filter set (Chroma) and a cooled CCD camera (Photometrics, Tucson, AZ), controlled by MetaFluor 2.75 software (Universal Imaging, West Chester, PA).

*Adenovirus construction.* To create adenoviruses expressing IFP1.1 or mKate and GFP, a transcription unit comprising the IFP1.1 or mKate coding sequence, the poliovirus IRES, and GFP was constructed by assembly PCR, cloned into pENTR1a (Invitrogen), and transferred into pAd-CMV-DEST (Invitrogen) by Gateway recombinase (Invitrogen). Viruses were produced in HEK293 cells by transfection followed by one round of amplification, purified by anion exchange chromatography (FastTrap purification kit, Millipore), resuspended in HBSS + 10% glycerol, and stored in aliquots at -80°C. Titers as assessed on HEK293 cells by GFP fluorescence were  $5 \times 10^{10}$  infectious units (IU) per mL for each virus.

*Mouse imaging.* The University of California San Diego Institutional Animal Care and Use Committee approved the protocol. Albino C57BL/6 mice (Jackson Labs) were injected with  $2 \times 10^9$  infectious units of adenovirus via tail vein. After 5 days, belly fur was removed using a depilatory cream. Mice were imaged on a spectral imager (Maestro,

Cambridge Research Instruments). The IFP channel was excited with a 650/50 nm (center wavelength/full width at half maximum) bandpass filter with a 700 nm long pass filter in series with the imager's tunable emission filter at 710/40 nm. The mKate channel was 590/24 nm bandpass for excitation and 620/20 in series with 630/40 nm for emission. Images for GFP were acquired with 467/45nm excitation and a 515 nm long pass filter in series with the imager's 530/40 nm for emission. Images were taken with 3 seconds exposure. Images for Fig. 3A were acquired before BV and 1 hr after injection of 250 nanomoles of BV, then scaled so that the brightest pixels after BV administration would display at maximum intensity. mKate and GFP images were first scaled with the same parameters as the IFP images, then the mKate images were further brightened 5-fold to make them visible. For fluorescence time course measurement, background-subtracted images of averaged liver intensity of the same region over liver at different time points after 250 nmole biliverdin injection was divided by the fluorescence intensity after 1 hour (Image J, NIH).

For spectral deconvolution, an image cube was collected on the Maestro with excitation at 620/20 nm and emission at 650-800 nm taking an image every 10 nm. Fluorescence region and autofluorescence regions were identified and spectrally unmixed using the instrument's software, revealing true fluorescent protein signal (displayed in red) and autofluorescence (displayed in grey).

For fluorescence molecular tomographic imaging (FMT), an Ad5I infected mouse was anesthetized with ketamine and midazolam, then injected IV with 250 nmole biliverdin in 10% DMSO. One hour later, the mouse was placed in a FMT 2500 imaging system (VisEn Medical, Bedford MA) and imaged in channel 1 with Prosense 680

settings. Images were reconstructed and windowed (106 – 167 nM apparent concentrations depicted in blue to red pseudocolors) to show the 3D distribution of fluorescence viewed from two different angles (Fig. S9).

After sacrifice, the mice were dissected and imaged using both IFP and mKate filter sets at 3 levels during dissection: with the skin on, with the skin removed, and then with the peritoneum and rib cage removed. Using Image J software, regions of 80x300 pixels were selected from below the liver up to the mid thorax. These regions were analyzed by plotting the profile. The values were normalized by dividing each pixel by the average of the last 30 vertical pixels over the thorax. These data represent contrast of liver to adjacent thoracic background.

*Liver histology.* Livers were frozen for cryohistology to compare fluorescence protein signal strength and relative expression. Sections were cut at 10  $\mu$ m and then imaged on a fluorescence stereomicroscope (Lumar, Zeiss). Filter sets used were ex 470/40 nm and em 525/50 nm for GFP, ex 560/25 nm and em 607/36 for mKate, and ex 665/45 and em 725/50 for IFP. Images were acquired at 15s exposures for IFP and mKate channels and 3s exposure for the GFP channel, then displayed with intensity enhancements of 2, 1, and 1 respectively. Therefore the relative gains for the IFP, mKate, and GFP channels were 10, 5, and 1 respectively.

## SOM Text

*Evolution of IFP1.4.* Random mutagenesis of IFP1.1 with fluorescence activated cell sorting using a 676 nm laser resulted in IFP1.2 with 32% increase in quantum yield (QY),

due to an additional M54V mutation. However, the parent of IFP1.2, *DrCBD*, was previously shown to be a dimer. Multiple angle light scattering at 785 nm (Dawn 8+, Wyatt Technology, Santa Barbara CA) of IFP1.2 gave an apparent molecular weight 80 kDa, about twice the predicted monomeric size of 36.5 kDa, suggesting that IFP1.2 was also a dimer. To monomerize IFP1.2, Leu311 was rationally mutated to a lysine since it is in the hydrophobic dimer interface based on the crystal structure of *DrCBD* (Fig. S3). Size exclusion chromatography (SEC) showed that the resulted mutant (named as IFP1.3) was eluted later than IFP1.2 (Fig. S3B), suggesting that IFP1.3 is possibly a monomer. SEC of IFP1.2/IFP1.3 mixture confirmed the result (Fig. S3B). However, the QY of IFP1.3 was slightly decreased (8%). Another round of random mutagenesis and screening generated IFP1.4 with increased brightness. SEC (Fig. S2) and multiple angle light scattering at 12 μM concentration (apparent molecular weight 41.5 kDa ± 10%) confirmed that IFP1.4 is monomeric. A sequence alignment of IFP1.4 with *DrCBD* is shown below with internal mutations shaded in blue. The S2A mutation (shaded in red) is to optimize the Kozak sequence when expressed in mammalian cells, and the C-terminal hexahistidine motif is to enable immobilized metal ion affinity chromatography.

<i>DrCBD</i>	MSRDPLPFFPPLYLGGPEITTENCEREPHIIPGSIQPHGALLTADGHSGEVLQMSLNAAT	60
IFP1.4	M <span style="background-color: red;">R</span> DPLPFFPPLYLGGPEITTENCEREPHIIPGSIQPHGALLTADGHSGEVLQ <span style="background-color: red;">V</span> SLNAAT	60
<i>DrCBD</i>	FLGQEPTVLRGQTLAALLPEQWPALQAAALPPGCPDALQYRATLDWPAAGHLSLTVHRVGE	120
IFP1.4	FLGQEPTVLRGQTLAALLPEQWPALQAAALPPGCPDALQYRATLDWPAAGHLSLTVHRV <span style="background-color: blue;">A</span> E	120
<i>DrCBD</i>	LLILEFEPTEAWDSTGPHALRNAMFALESAPNLRALAEVATQTVERLTGFDRVMLYKFAP	180
IFP1.4	LLILEFEPTEAWDS <span style="background-color: blue;">I</span> GPHALRNAMFALESAPNLRALAEVATQTVERLTGFDRVMLYKFAP	180
<i>DrCBD</i>	DATGEVIAEARREGLHAFLGHRFPASDI <span style="background-color: blue;">P</span> AQARALYTRHLLRLTADTRAACVPLDPVLNP	240
IFP1.4	DATGEMIAEARREG <span style="background-color: blue;">M</span> OFLGHRFPAS <span style="background-color: blue;">H</span> TPAQARALYTRHLLRLTADTRAACVPLDPVLNP	240
<i>DrCBD</i>	QTNAPTPLGGAVLRLATSPMHMQYLRLNMVGSSLSVSVVVGQLWGLIACHHQTPYVLPPD	300
IFP1.4	QTNAPTPLGGAVLRLATSPMHMQYLRLNMVGSSLSVSVVVGQLWGLIV <span style="background-color: blue;">C</span> HHQTPYVLPPD	300
<i>DrCBD</i>	LRTTLEYLGRLLSLQVOVKEA	321
IFP1.4	LRTTLE <span style="background-color: blue;">E</span> LGRL <span style="background-color: blue;">K</span> LSG <span style="background-color: blue;">Q</span> VQRKEA <span style="background-color: blue;">EFHHHHHH</span>	329

*Increase of cellular IFP fluorescence by exogenous BV.* HEK293A cells were transiently transfected with IFP1.4 in one 10-cm dish and incubated for 24 hours, trypsinized and replated into 5 wells of 6-well plate with ~ 400,000 cells per well. After another 24 hours incubation, different amounts of BV (final concentrations 5, 10, 20, 40  $\mu$ M) were added, followed by 90 minutes incubation. Then cells were trypsinized and washed with PBS and resuspended for fluorescence measurement by a 96-well plate reader with monochromators (Safire, TECAN). Untransfected HEK293A cells with additions of exogenous BV were used as controls. Infrared fluorescence of transfected HEK293A cells increased upon the increase of added exogenous BV concentration and was saturated at 20  $\mu$ M, while the untransfected cells did not show infrared fluorescence either with or without BV (Fig. S6A). Addition of exogenous BV rapidly (within 10 minutes) led to infrared fluorescence of matured P2 cortical neurons, two weeks after transfection of IFP1.1 (Fig. S6B), which were practically nonfluorescent before addition of BV.

*Half-life of IFP1.4.* Cycloheximide (30  $\mu$ g/ml final concentration) was added to HEK293A cells 24 hours after transfection of IFP1.4. Infrared fluorescence was fitted with single exponential decay assuming first-order decay kinetics of protein degradation (S5) (Figs. S7 and S8). The half-life of IFP1.4 in HEK293A cells with or without exogenous BV was calculated to be 4.44 and 3.61 hours, whose average is  $4.03 \pm 0.41$  hours.

*Multiple sequence alignment.* 130 bacteriophytochrome-like sequences from NCBI database are aligned using *DrCBD* as the query (*S6*). Readers are suggested to zoom in to read the alignment.













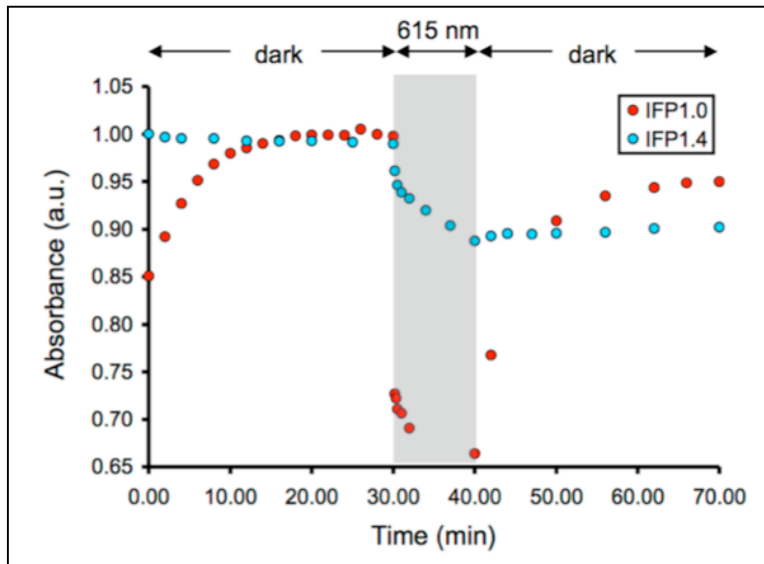


**Fig. S1** Dark and light adapted behavior of IFP1.0 and IFP1.4. Absorbance spectra at different time points were taken in the dark (0 – 30 min.), upon 615 nm light illumination by solar simulator (30 – 40 min.), and then in the dark again (40 – 70 min.).

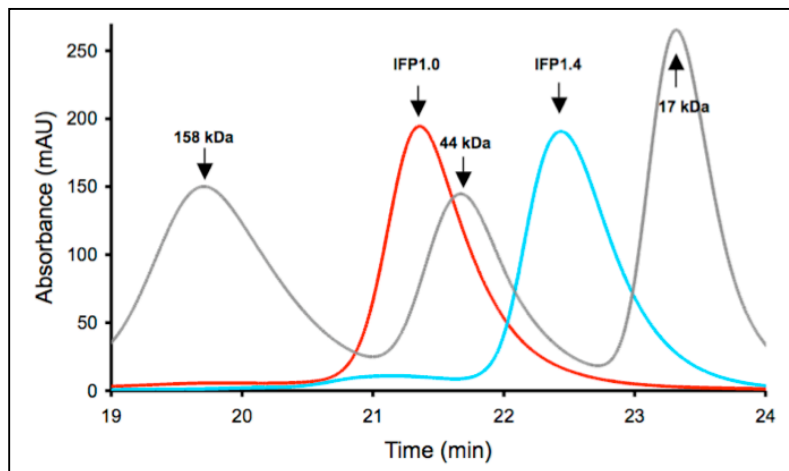


**Fig. S2** Size exclusion chromatography of IFP1.0 and1.4. Three standards are also shown:  $\gamma$ -globulin (158 kDa), ovalbumin (44 kDa) and myoglobin (17 kDa). Absorbance was measured at 280 nm.

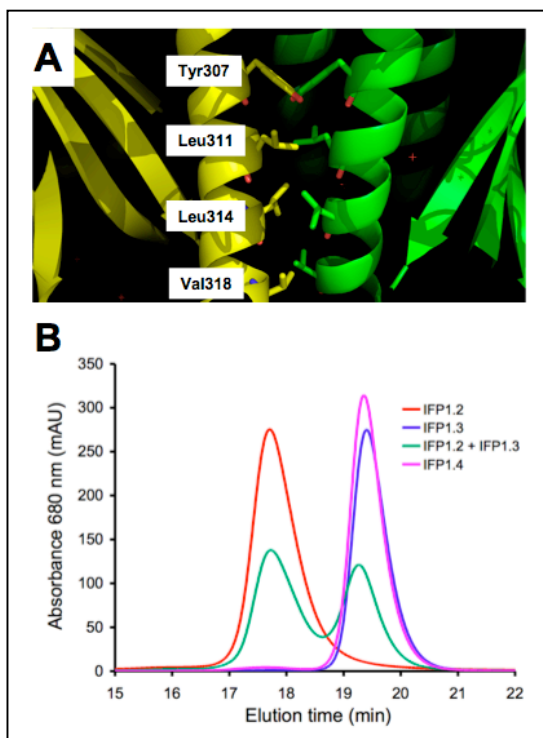


**Fig. S3** IFP monomerization by L311K mutation. (A) The dimer interface in DrCBD is formed from 4 residues (Y307/L311/L314/V318). (B) Size exclusion chromatography of IFP1.2, 1.3, 1.4 and a mixture of IFP1.2 and 1.3.

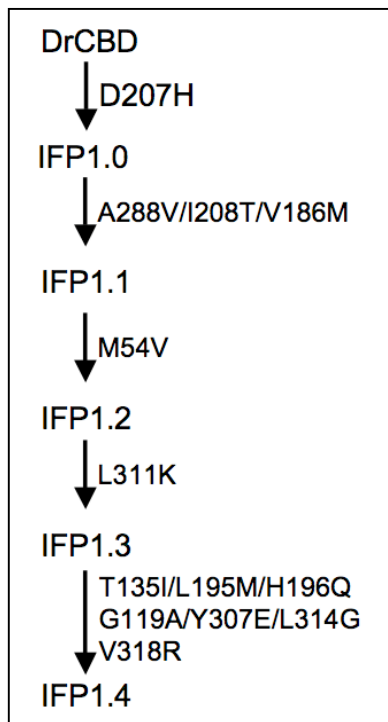


**Fig. S4** Evolution of IFPs showing the mutations introduced at each stage. .

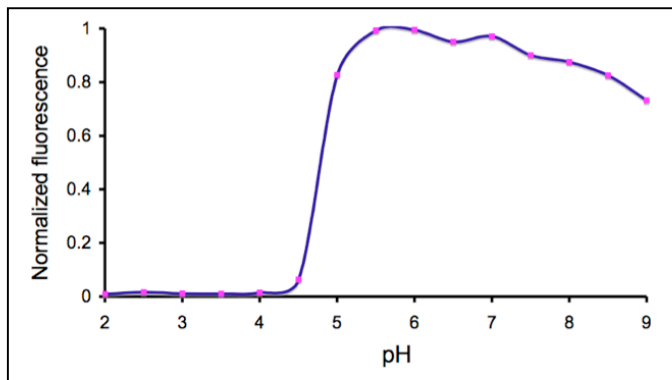


**Fig. S5** pH dependence of IFP1.4 fluorescence. IFP1.4 was excited at 640 nm and its emission at 700 - 800 nm was integrated, normalized and plotted against pH.

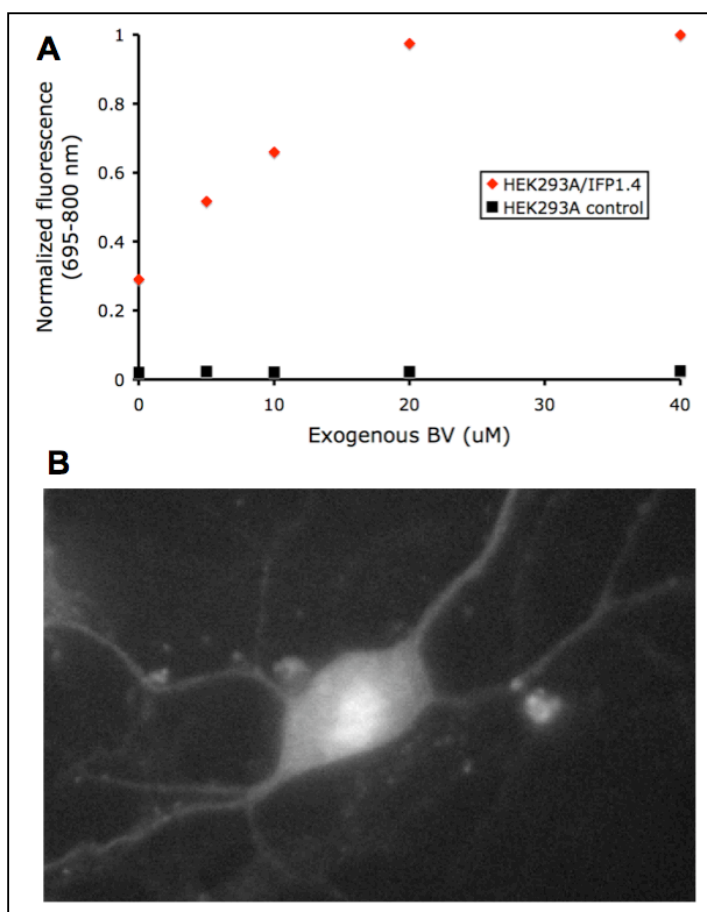


**Fig. S6** Increase of IFP fluorescence by addition of exogenous BV. **(A)** IFP1.4-transfected HEK293A cells indicated increase of fluorescence upon addition of exogenous BV, with untransfected cells as the control. IFP fluorescence was integrated from 695 to 800 nm upon excitation at 660 nm. **(B)** Fluorescence image of a P2 cultured cortical neuron 2 weeks after transfection of IFP1.1, 10 minutes after addition of 25 uM BV.

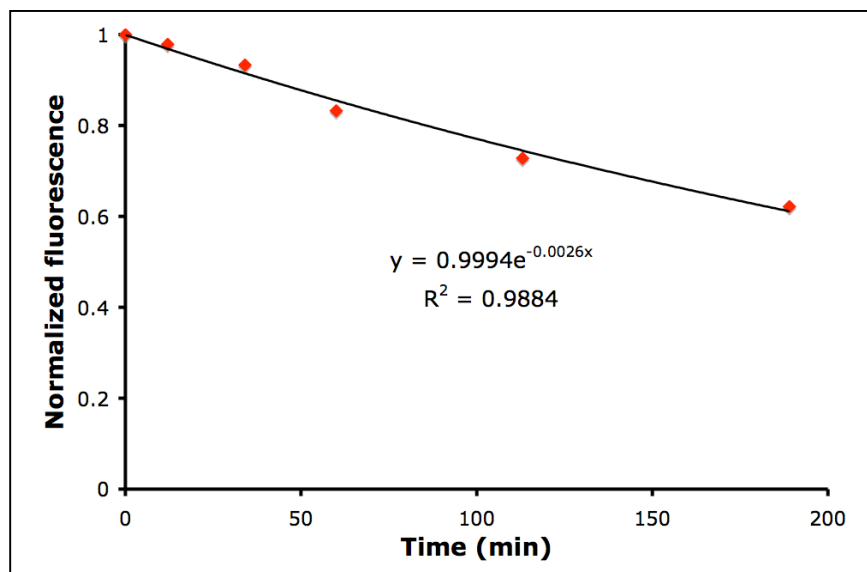


**Fig. S7** IFP1.4 degradation in HEK293A cells with 20uM BV added.

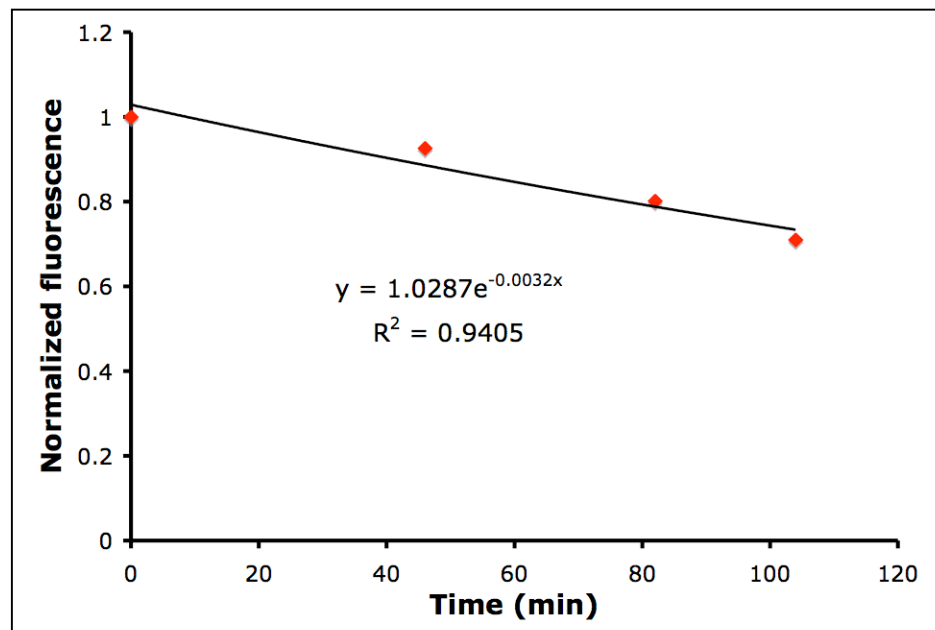


**Fig. S8** IFP1.4 degradation in HEK293A cells without exogenous BV.

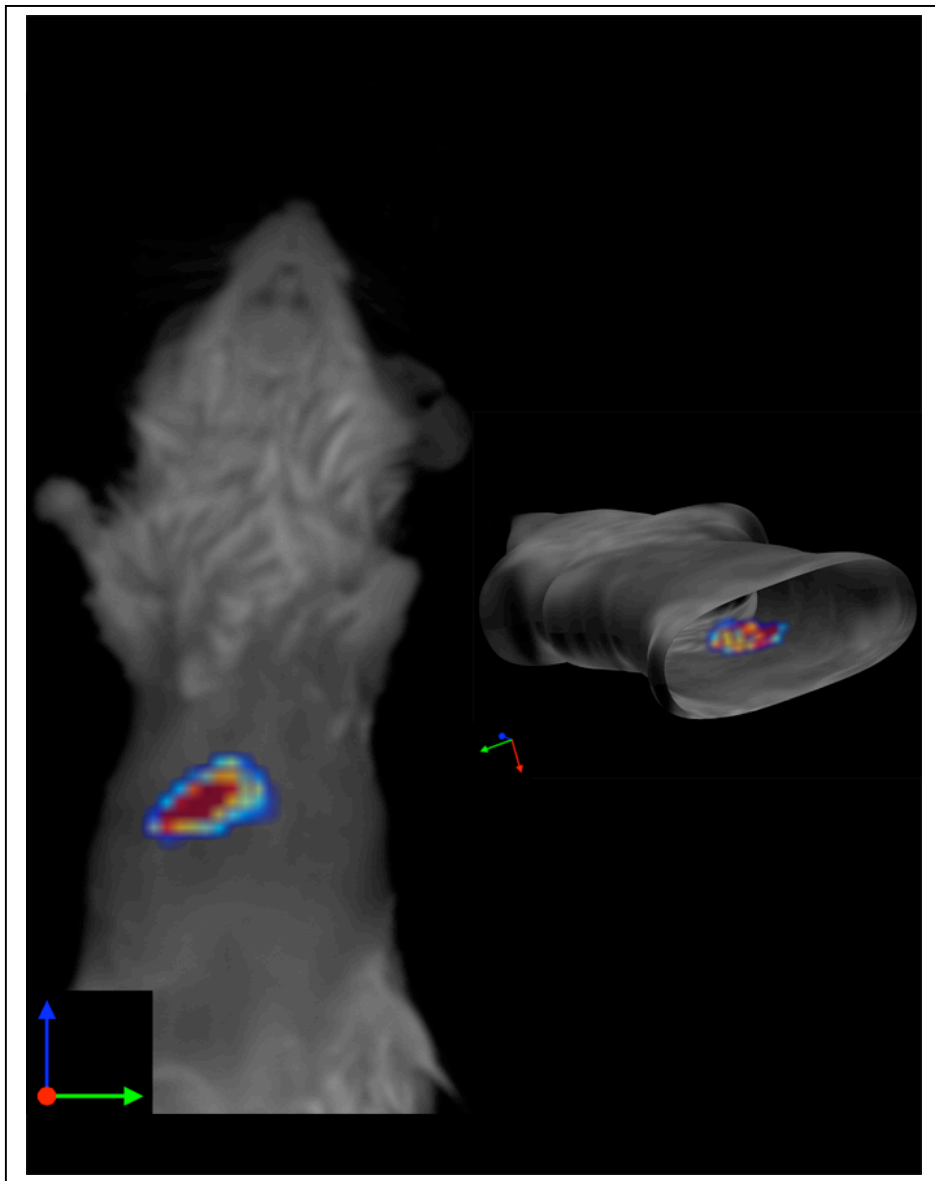


**Fig. S9** Noninvasive fluorescence molecular tomographic (FMT) imaging of IFP-expressing mouse liver. Blue, green, and red arrows indicate rostral-caudal, left-right, and dorsoventral axes respectively. Left: top view. Right: tilted view to show the 3D localization of fluorescence within the mouse.

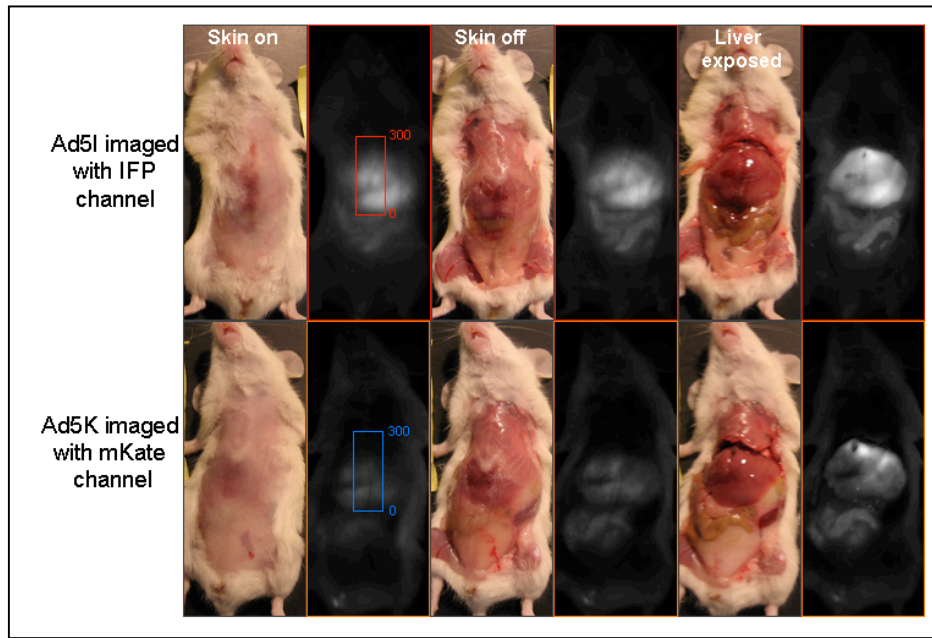


**Fig. S10** IFP/mKate fluorescence images before dissection (skin on), after removal of skin (skin off), and after removal of overlying peritoneum and ribcage (liver exposed). mKate images were 2.5X brightened relative to IFP images. Note that Ad5I infected mouse was imaged after 250 nmole IV injection of BV.

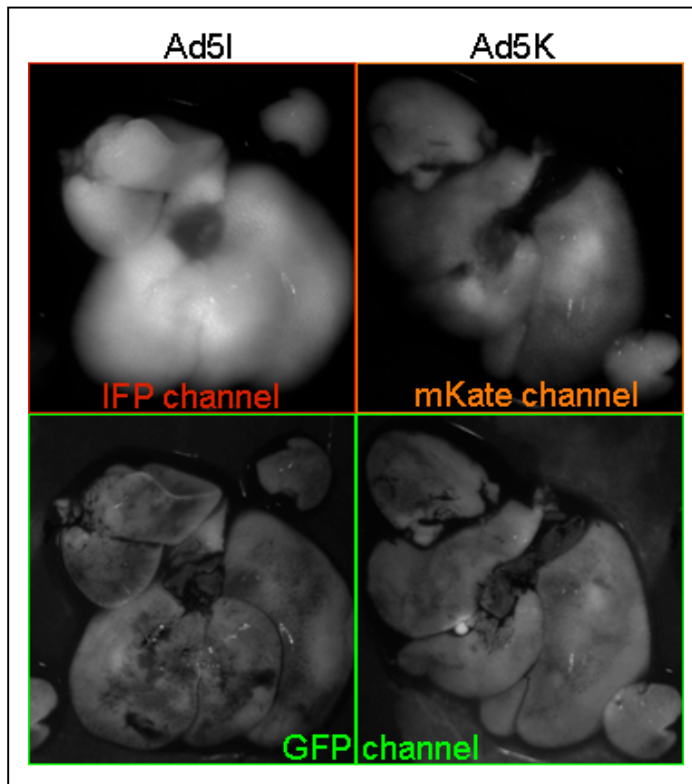


**Fig. S11** Imaging of extracted livers infected with Ad5I and Ad5K.

**Table S1 Properties of infrared fluorescent protein variants.**

Fluorescent protein	Absorption max. (nm)	Extinct. coeff. (M <sup>-1</sup> cm <sup>-1</sup> )	Emission max. (nm)	Quantum yield	Relative brightness (%)	Stoichiometry
IFP1.0	699	60,000	722	0.028	100	Dimer
IFP1.1	686	86,000	713	0.050	256	Dimer
IFP1.2	684	86,000	707	0.066	338	Dimer
IFP1.3	684	84,000	707	0.061	305	Monomer
IFP1.4	684	92,000	708	0.070	383	Monomer

## Supporting References

- S1. W. P. C. Stemmer, A. Crameri, K. D. Ha, T. M. Brennan, H. L. Heyneker, *Gene* **164**, 49 (1995).
- S2. N. C. Shaner *et al.*, *Nat. Biotechnol.* **22**, 1567 (2004).
- S3. W. P. C. Stemmer, *Nature* **370**, 389 (1994).
- S4. R. B. Mujumdar, L. A. Ernst, S. R. Mujumdar, C. J. Lewis, A. S. Waggoner, *Bioconjug. Chem.* **4**, 105 (1993).
- S5. A. Belle, A. Tanay, L. Bitincka, R. Shamir, E. K. O'Shea, *Proc. Natl. Acad. Sci. U.S.A.* **103**, 13004 (2006).
- S6. S. F. Altschul *et al.*, *Nucleic Acids Res.* **25**, 3389 (1997)